The American Journal of Pathology, Vol. 191, No. 4, April 2021

The American Journal of
PATHOLOGY
ajp.amjpathol.org

SHORT COMMUNICATION

Enzymatically Inactive Tissue-Type Plasminogen Activator Reverses Disease Progression in the Dextran Sulfate Sodium Mouse Model of Inflammatory Bowel Disease

Lipsa Das, Michael A. Banki, Pardis Azmoon, Donald Pizzo, and Steven L. Gonias

From the Department of Pathology, University of California San Diego, La Jolla, California

Accepted for publication January 6, 2021.

Address correspondence to Steven L. Gonias, M.D., Ph.D., Department of Pathology, University of California San Diego, 9500 Gilman Dr., #0612, La Jolla, CA 92093. E-mail: sgonias@health.ucsd.edu.

Enzymatically inactive tissue-type plasminogen activator (EI-tPA) does not activate fibrinolysis, but interacts with the N-methyl-D-aspartate receptor (NMDA-R) and low-density lipoprotein receptor–related protein-1 (LRP1) in macrophages to block innate immune system responses mediated by toll-like receptors. Herein, we examined the ability of EI-tPA to treat colitis in mice, induced by dextran sulfate sodium. In two separate studies, designed to generate colitis of differing severity, a single dose of EI-tPA administered after inflammation established significantly improved disease parameters. EI-tPA–treated mice demonstrated improved weight gain. Stools improved in character and became hemoccult negative. Abdominal tenderness decreased. Colon shortening significantly decreased in EI-tPA–treated mice, suggesting attenuation of irreversible tissue damage and remodeling. Furthermore, histopathologic evidence of disease decreased in the distal 25% of the colon in EI-tPA–treated mice. EI-tPA did not decrease the number of CD45-positive leukocytes or F4/80-positive macrophage-like cells detected in extracts of colons from dextran sulfate sodium–treated mice as assessed by flow cytometry. However, multiple colon cell types expressed the NMDA-R, suggesting the ability of diverse cells, including CD3-positive cells, CD103-positive cells, Ly6G-positive cells, and epithelial cell adhesion molecule–positive epithelial cells to respond to EI-tPA. Mesenchymal cells that line intestinal crypts and provide barrier function expressed LRP1, thereby representing another potential target for EI-tPA. These results demonstrate that the NMDA-R/LRP1 receptor system may be a target for drug development in diseases characterized by tissue damage and chronic inflammation. *(Am J Pathol 2021, 191: 590–601; https://doi.org/10.1016/j.ajpath.2021.01.001)*

The inflammatory bowel diseases (IBDs), such as Crohn disease and ulcerative colitis, are chronic, relapsing diseases of the intestines that eventually compromise tissue structure and function.[1] Disease susceptibility genes such as the pattern recognition receptor, nucleotide-binding oligomerization domain containing 2 (NOD2), have been implicated in Crohn disease.[1,2] Dysbiosis in intestinal microbiomes also has been implicated in the onset of IBD, together with lifestyle choices, such as cigarette smoking.[3–5] Once IBD is established, chronic inflammation and tissue damage dominate the clinical course and are principal targets for therapeutics development.[6] Despite the availability of numerous drugs, many patients with moderate to severe IBD fail to remain in remission and often experience damaging flares.

Tissue-type plasminogen activator (tPA) is a serine protease and major activator of the fibrinolytic system.[7,8] Recombinant tPA is Food and Drug Administration-approved for treating recent-onset stroke.[9] The structure of tPA

Supported by NIH grant R01 HL136395 (S.L.G.).
Disclosures: None declared.
Current address of L.D., University of Arizona Cancer Center, Tucson, AZ.

https://doi.org/10.1016/j.ajpath.2021.01.001

includes multiple domains that participate in noncovalent fibrin binding, which is essential for restricting the lytic activity of tPA to fibrin while sparing fibrinogen.[10–12] tPA also binds to cell surface receptors, including the N-methyl-D-aspartate receptor (NMDA-R) and low-density lipoprotein receptor–related protein-1 (LRP1), which function as part of a single system to regulate cell signaling and cell physiology.[13–17] Enzymatically inactive tPA (EI-tPA), in which the enzyme active site serine is mutated to alanine, interacts with the NMDA-R/LRP1 receptor system equivalently to enzymatically active tPA to trigger signal transduction.[16,18,19]

In mouse macrophages, EI-tPA binding to the NMDA-R/LRP1 receptor system blocks inflammatory cytokine expression elicited by multiple toll-like receptors (TLRs), including TLR4, TLR2, and TLR9.[18–20] EI-tPA also blocks the toxicity of lipopolysaccharide *in vivo* in mice.[18] These results suggest that EI-tPA and the NMDA-R/LRP1 receptor system constitute a novel pathway for regulating innate immunity and inflammation. EI-tPA does not activate plasminogen, thus avoiding undesirable effects on hemostasis and the possible proinflammatory activity of plasmin.[21,22] Some pattern recognition receptors outside the TLR family, such as NOD1 and NOD2, are not antagonized by EI-tPA in macrophages.[19] Furthermore, because the NMDA-R is expressed by numerous cell types,[17,18,23,24] EI-tPA may regulate inflammation by targeting cells in addition to macrophages. Thus, it is not clear whether EI-tPA would be effective in counteracting pathologic conditions in which diverse pattern recognition receptors function together in diverse cells to stimulate fulminant inflammation.

In this study, the dextran sulfate sodium (DSS) preclinical mouse model of colitis was used to test the activity of EI-tPA. DSS causes a chemically-induced form of colitis, in which extensive inflammatory cell infiltrates develop in the mucosa and submucosa.[25] Mice were treated systemically with a single dose of EI-tPA after intestinal inflammation was established. EI-tPA rapidly reversed signs and symptoms of the disease and caused significant improvement in disease biomarkers. These results indicate that EI-tPA may be efficacious as a therapeutic for complex inflammatory diseases.

Materials and Methods

DSS Challenge in Mice

Experimental procedures involving animals were approved by the University of California San Diego Institutional Animal Care and Use Committee. Male C57BL/6 mice, aged 7 to 8 weeks (weight, 18 to 24 g), were obtained from Jackson Laboratory (Bar Harbor, ME). Mice were randomly sorted into cohorts, and provided ad libitum access to standard drinking water or water supplemented with DSS (approximately 40 kDa; Sigma-Aldrich, St. Louis, MO). DSS was administered in two different protocols to model colitis of moderate severity (4% DSS w/v for 5 days) or severe colitis (5% DSS w/v for 7 days). Fresh DSS was replaced in the drinking water every 48 hours or if cloudiness was observed. On the final day of DSS exposure, half of the mice were treated with a single i.v. injection of EI-tPA (2.5 mg/kg) and the other half were injected with vehicle (20 mmol/L sodium phosphate and 150 mmol/L NaCl, pH 7.4). DSS-containing water was replaced with unaltered water, and the mice were monitored for up to 7 additional days. In control studies, mice that were not exposed to DSS were injected with EI-tPA. Human EI-tPA, which carries the S478→A mutation and is 90% in the single-chain form, was obtained from Molecular Innovations (Novi, MI). Human EI-tPA and mouse EI-tPA engage the mouse NMDA-R/LRP1 receptor system and inhibit TLR responses equivalently.[18]

Assessment of Symptoms in DSS-Treated Mice

Mice were monitored daily for changes in body weight, stool consistency, diarrhea, and fecal blood. Stools were scored by a blinded investigator as follows: 0, normal stool consistency with a negative hemoccult; 1, soft stools with a negative hemoccult; 2, soft stools with a positive hemoccult; 3, watery stools with visible blood; and 4, gross rectal bleeding.

Analysis of Abdominal Tenderness

Abdominal tenderness was assessed by the response to calibrated von Frey filaments.[26] Baseline testing was conducted for 3 days before DSS exposure. Testing was repeated after terminating DSS treatment, on day 5, and on day 11. All testing was conducted at a fixed time of day in a quiet dedicated room by the same blinded experimenter (L.D.). After 1 hour of acclimatization, mice were placed in individual Plexiglas chambers (6 × 10 × 12 cm). Eight individual von Frey filaments, with forces ranging from 0.19 to 19 mN (Stoelting, Wood Dale, IL), were applied in ascending order of force for 1 to 2 seconds to the lower left abdominal quadrant with at least 5-second intervals between stimulations. Each filament was tested six times. Mice were considered to have responded if any of the following behaviors was observed: i) retraction of the abdomen; ii) immediate licking or scratching of the area of stimulation; or iii) withdrawal of the animal. When the response frequency to an individual filament was >50%, the response was recorded as positive.

Tissue Harvest

Mice were euthanized by CO_2 inhalation and cervical dislocation. The large intestines were harvested intact by resecting at the ileocecal valve and at the rectum. Colon length was measured. The cecum was removed, the colon was cut longitudinally, fecal material was removed, and the

tissue was flushed extensively with saline. Harvested colons were used to collect intestinal cells or studied by histology. For histology, longitudinally cut colons were Swiss rolled and fixed in 4% paraformaldehyde.

Histology and Immunohistochemistry

Tissue sections (4 μm thick) were prepared and stained with hematoxylin and eosin. For immunohistochemistry, tissue sections were stained using the Discovery Ultra automated system (Roche, Basel, Switzerland). Sections were deparaffinized, subjected to antigen retrieval, then incubated with primary antibody against LRP1 β-chain (Sigma-Aldrich) or CD11b (Abcam, Cambridge, UK), followed by horseradish peroxidase—coupled goat anti-rabbit antibodies, and developed using diaminobenzidine. Control sections were treated with secondary antibody only. Light microscopy was performed using a Leica DFC420 microscope with Leica Imaging Software 2.8.1 (Leica Biosystems, Wetzlar, Germany).

Scoring Histopathologic Changes in DSS-Treated Colons

Swiss-rolled hematoxylin and eosin—stained colon sections were scored by a blinded investigator (M.A.B. and S.L.G.), as described by Erben et al.[27] Because the pathologic changes induced by DSS were segmental with skip lesions, scoring was restricted to the distal 25% of the colon. Epithelial changes were scored as follows: 0, no noticeable changes; 1, minimal hyperplasia; 2, moderate hyperplasia, goblet cell loss, and crypt abscesses; and 3, marked hyperplasia, goblet cell loss, and multiple crypt abscesses or erosions. Infiltration of inflammatory cells was scored as follows: 0, negligible infiltration; 1, infiltration of the mucosa; 2, infiltration of the mucosa and submucosa; and 3, transmural infiltration.

Isolation of Intestinal Cells

A mild method was applied to isolate cells, which primarily included epithelial cells and cells in the lamina propria. Each colon was processed separately. The cecum was removed, and mesenteric fat was resected. The remaining colon tissue was cut into 0.5- to 1.0-cm^2 pieces and treated with 5 mmol/L EDTA in 10 mmol/L HEPES-buffered Ca^{+2}/Mg^{+2}-free Hanks' balanced salt solution at 37°C for 20 minutes to dissociate cells. Cell suspensions were filtered through 70-μm nylon meshes and transferred into Dulbecco's modified Eagle's medium supplemented with 10% fetal bovine serum and 1× antibiotic/antimycotic solution (Sigma-Aldrich). The EDTA dissociation protocol was repeated twice, and the cells were pooled. Cells were pelleted by centrifugation at 400 × *g* for 10 minutes and resuspended for flow cytometry.

A more rigorous colon cell isolation method was executed to harvest residual cells after EDTA extraction. Specimens were digested with 1 mg/mL collagenase/dispase cocktail (Sigma-Aldrich) in Ca^{2+}/Mg^{2+}-free Hanks' balanced salt solution at 37°C for 30 minutes with intermittent vortexing. The process was repeated twice. Cell suspensions were pooled and passed through a 70-μm nylon mesh. Cells were pelleted by centrifugation at 400 × *g* for 10 minutes and resuspended for flow cytometry.

Flow Cytometry

Cells were isolated from colons. Non-specific IgG binding was blocked by pretreating cells with antibody against Fc-γ receptor (clone 2.4G2; Bio X Cell, Lebanon, NH). Cells were pre-incubated with Zombie NIR (BioLegend, San Diego, CA) for 10 minutes to identify viable cells. Next, cells were labeled with Brilliant Violet 421—conjugated antibody against CD45 (clone 30-F11; BD Biosciences, San Jose, CA) to label leukocytes and phycoerythrin-conjugated antibody against epithelial cell adhesion molecule (EpCAM; clone G8.8; eBioscience, San Diego, CA) to label epithelial cells. CD45-positive cells were further sorted using fluorescein isothiocyanate—conjugated F4/80-specific antibody (clone BM8; BioLegend), which detects macrophages and macrophage-related cell types.[28] Sorting was performed using a BD FACSAria Fusion Cell Sorter (BD Biosciences).

To detect cell-surface NMDA-R in specific colon cell populations by flow cytometry, cells were labeled with antibody PA3-102 (Thermo Fisher Scientific, Waltham, MA), which detects the glutamate ionotropic receptor NMDA type subunit 1 (GluN1) NMDA-R subunit. GluN1 is essential for formation of intact NMDA-Rs.[29] Cell-associated PA3-102 was detected with A647- or A488-conjugated secondary antibody (Thermo Fisher Scientific). Control cells were treated with secondary antibody only. Cells that were incubated with PA3-102 were colabeled with conjugated CD45 antibody or EpCAM antibody and, in some studies, with A488-conjugated antibodies against CD3, CD103, or Ly6G (BioLegend). All data were analyzed using FlowJo Software version 10.7.1 (BD Biosciences).

Statistical Analysis

All results are expressed as the means ± SEM. The one- or two-way analysis of variance was performed with a post-hoc Bonferroni test using GraphPad Prism version 9.0 (GraphPad Software, San Diego, CA). P values of $^*P < 0.05$, $^{**}P < 0.01$, $^{***}P < 0.001$, and $^{****}P < 0.0001$ were considered statistically significant.

Results

EI-tPA Reverses DSS-Induced Colitis in a Model of Moderate Severity Disease

Eight-week—old C57BL/6 male mice were exposed to 4% DSS in the drinking water for 5 days, after which DSS-free

drinking water was provided. Control mice received DSS-free drinking water throughout the study. A single dose of EI-tPA (2.5 mg/kg) or vehicle (phosphate-buffered saline) was administered by i.v. injection on day 5. The EI-tPA dose was about 2.5× the dose of active tPA recommended for human patients with stroke (0.9 mg/kg).[9] Control mice demonstrated weight gain throughout the study (Figure 1A). In control mice injected with EI-tPA on day 5, the mean weight on day 12 was not significantly different than that observed in mice injected with vehicle. By contrast, significant weight loss was observed in DSS-treated mice beginning on day 5 and continuing through day 7, 2 days after terminating the DSS, when weight loss apparently stabilized. A single dose of EI-tPA, administered on day 5 to DSS-treated mice, significantly improved weight gain, when measured on days 10 through 12.

A scoring system was applied to quantify the effects of DSS on the stools of mice. After 5 days of DSS treatment, the mean stool abnormality score was slightly <3.0, implying watery hemoccult-positive stools (Figure 1B). After discontinuing DSS treatment, stool scores began to improve; however, in the absence of EI-tPA, abnormally soft stools persisted through day 11. EI-tPA treatment significantly accelerated the rate of improvement in the stool score.

Abdominal tenderness was examined by probing the abdomen with von Frey filaments. The mice exposed to DSS responded to filaments of lower force compared with control mice, indicating abdominal tenderness (Figure 1C). For example, on day 5, only 10% of the mice in the control group (no DSS exposure) responded positively to a 1.6-mN force von Frey filament, whereas 90% of the DSS-treated mice responded positively to the same filament. By day 11, DSS-exposed mice demonstrated partial recovery (less abdominal tenderness); however, a much more substantial recovery was observed in mice treated with EI-tPA on day 5.

Next, colon length was measured as a marker of disease progression, irreversible tissue damage, and scarring. Mice exposed to 4% DSS for 5 days and then treated with EI-tPA or vehicle, and control mice (no DSS treatment) were euthanized on day 12. Figure 1D shows representative colons harvested from mice in each cohort. The results of seven independent studies are summarized in Figure 1E. Significant colon shortening was observed in DSS-exposed versus that in control mice. EI-tPA significantly decreased the extent of colon shortening, compared with mice treated with vehicle. EI-tPA had no effect on intestinal length when administered in the absence of DSS (results not shown).

Mice exposed to 4% DSS for 5 days and euthanized on day 12 demonstrated anticipated changes in colon histopathology.[23,30] Untreated control colon is shown in Figure 1F. The specimen was rolled so that the distal end of the colon was near the center of the slide. Uniform unperturbed intestinal crypts and epithelium with interspersed goblet cells were observed, as anticipated. In DSS-treated mice, segmental lesions separated by areas of less involved colon (skip lesions) were common (Figure 1G). Lesions were characterized by epithelial denudation and crypt disruption with extensive inflammatory cell infiltration surrounded by areas in which the crypts contained hyperplastic epithelium devoid of goblet cells.

In mice exposed to DSS and then treated with EI-tPA on day 5, segmental lesions with disrupted or absent crypts and extensive inflammation were still observed; however, there was evidence of repair, primarily at the distal end of the colon (Figure 1H). This result was confirmed by a blinded investigator (M.A.B. and S.L.G.) who applied a scoring system to evaluate the histopathology. Infiltrating cells (Figure 1I) and abnormalities in the epithelium (Figure 1J) were substantially increased by DSS treatment. In the most distal 25% of the colon, EI-tPA significantly improved both pathology scores. To confirm that the infiltrating cells in DSS-treated mice included inflammatory cells, tissue sections obtained from mice treated for 5 days with 4% DSS were immunostained for CD11b, which is expressed by monocytes, macrophages, dendritic cells, neutrophils, and natural killer cells.[31] CD11b-positive cells were observed in the mucosa and submucosa of colons exposed to DSS (Figure 1K).

EI-tPA Reverses DSS-Induced Colitis in a Model of Severe Disease

To model severe colitis, cohorts of mice were exposed to 5% DSS for 7 days. On day 7, DSS was removed from the water and the mice were treated with either EI-tPA (2.5 mg/kg) or vehicle. Control mice were not exposed to DSS. Mice treated with 5% DSS began to lose weight by day 5 (Figure 2A). In the absence of EI-tPA, weight loss continued through day 12, at which time weight recovery began to occur. Mice treated with EI-tPA showed significantly more rapid weight recovery.

Mice exposed to 5% DSS for 7 days demonstrated a mean stool abnormality score >3.0 (Figure 2B). Stool scores began to improve after discontinuing DSS treatment. In the absence of EI-tPA, persistent diarrhea and some positive hemoccults were observed through day 13. EI-tPA treatment significantly accelerated the rate of improvement in the stool score.

Representative colons isolated from mice on day 14 are shown in Figure 2C. Colon lengths are summarized in Figure 2D. Colons harvested from DSS-treated mice showed substantial shortening. A single dose of EI-tPA, administered on day 7, significantly decreased the degree of colon shortening.

Histopathologic examination of colons harvested on day 14 from mice treated for 7 days with 5% DSS demonstrated segmental lesions throughout, including the distal end, which is shown in the representative image (Figure 2E).

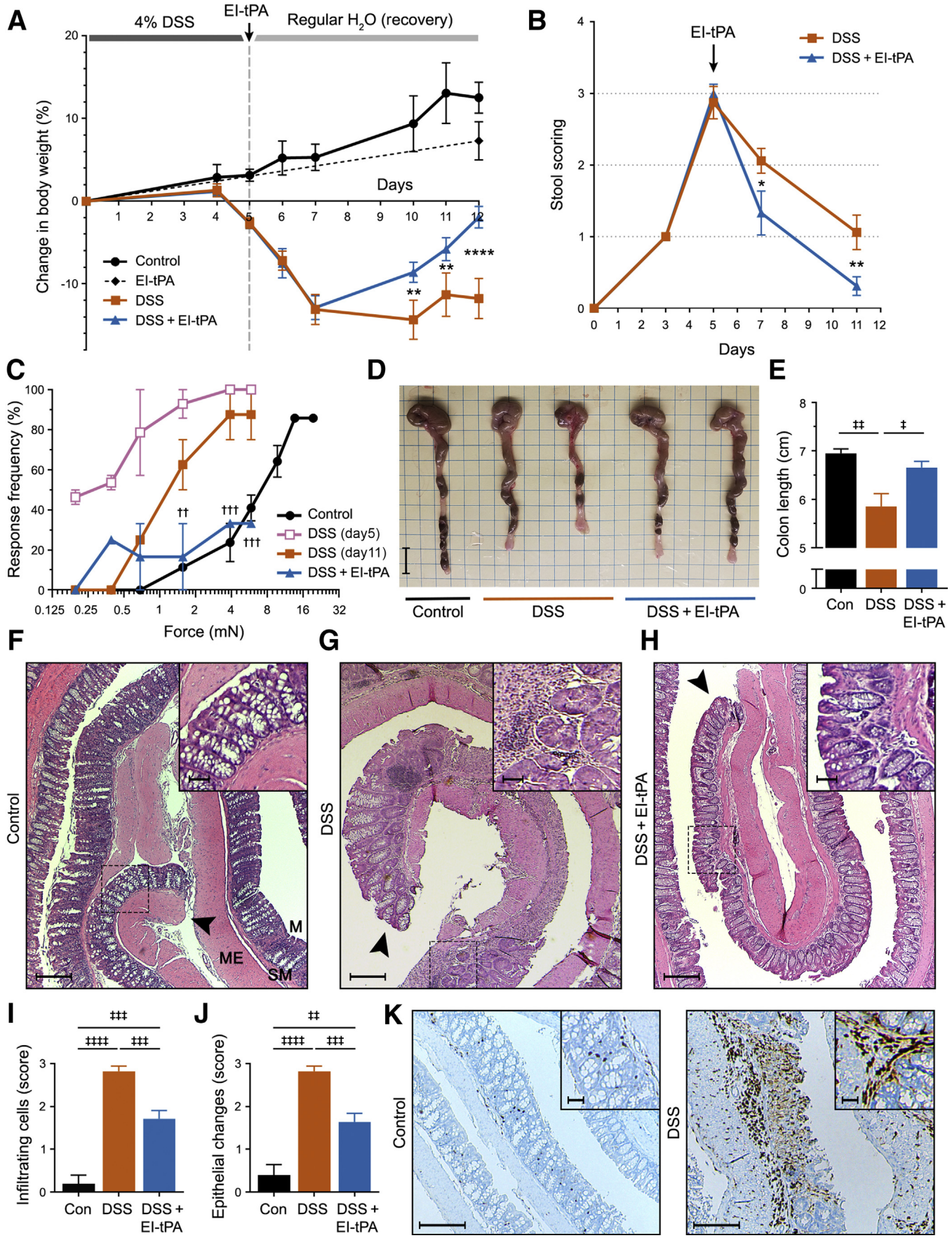
A
4% DSS
EI-tPA
Regular H2O (recovery)
Change in body weight (%)
Days
Control
EI-tPA
DSS
DSS + EI-tPA
B
EI-tPA
DSS
DSS + EI-tPA
Stool scoring
Days
C
Response frequency (%)
Force (mN)
Control
DSS (day5)
DSS (day11)
DSS + EI-tPA
D
Control
DSS
DSS + EI-tPA
E
Colon length (cm)
Con
DSS
DSS + EI-tPA
F
G
H
Control
DSS
DSS + EI-tPA
M
ME
SM
I
Infiltrating cells (score)
Con
DSS
DSS + EI-tPA
J
Epithelial changes (score)
Con
DSS
DSS + EI-tPA
K
Control
DSS

Lesions with crypt disruption and inflammation were observed in EI-tPA–treated mice; however, once again, there appeared to be fewer residual pathologic changes near the distal end of the colon (Figure 2F). This trend was confirmed by blinded scoring of infiltrating cells (Figure 2G) and epithelial abnormalities (Figure 2H) in the distal 25% of the specimens.

Inflammatory Cell Infiltration of Colons Is Increased by DSS and Unaffected by EI-tPA

Cells from intact, whole colons were isolated on day 12 after treating mice with 4% DSS for 5 days and then injecting them with EI-tPA or vehicle. Control mice were not DSS-exposed. EDTA-extracted cells were sorted using antibodies specific for epithelial cells (EpCAM) and leukocytes (CD45) (Figure 3A). CD45-positive cells were further sorted to detect F4/80-positive macrophages and macrophage-like cells (Figure 3C). The results of three independent experiments are summarized in Figure 3, B and D.

EpCAM-positive and CD45-positive cells were detected under all conditions. Cells that were neither CD45-positive nor EpCAM-positive were considered mesenchymal cells, as previously described.[32] DSS exposure increased the percentage of CD45-positive cells from 1.7% ± 0.3% to 11% ± 2%. The percentage of CD45-positive cells was not significantly changed in DSS-exposed mice treated with EI-tPA. In mice not exposed to DSS, 7% ± 4% of the CD45-positive cells were F4/80-positive. In DSS-exposed mice, the percentage of CD45-positive cells that were F4/80-positive increased to 24% ± 1%. EI-tPA treatment did not significantly affect this result.

Colons pre-extracted with EDTA were further extracted with collagenase. The second set of extracts was subjected to flow cytometry. Once again, both CD45-positive and EpCAM-positive cells were identified. Although DSS treatment significantly increased the fraction of CD45-positive cells, EI-tPA did not significantly affect this result (Figure 3, E and F).

Diverse Intestinal Cells Express the Receptors Required for EI-tPA Response

The NMDA-R is essential for many EI-tPA–initiated cellular responses, including regulation of innate immunity, whereas LRP1 functions as a coreceptor, possibly by delivering EI-tPA to the NMDA-R.[14–18,33] To test whether leukocytes from colons express the NMDA-R, CD45-positive cells were probed for GluN1 by flow cytometry. GluN1 is essential for the formation of NMDA-Rs.[29] In control mice, CD45-positive cells expressed GluN1, as determined by comparing the flow histograms of cells immunostained for GluN1 versus secondary antibody only (Figure 4A). A significant increase in the mean cell-surface abundance of GluN1 was observed in CD45-positive cells isolated from mice exposed to DSS and treated with either EI-tPA or vehicle (Figure 4B). EpCAM-positive epithelial cells also expressed cell-surface NMDA-R (Figure 4C). The abundance of cell-surface NMDA-R increased in epithelial cells from DSS-treated mice and, interestingly, further increased by EI-tPA (Figure 4D).

Next, flow cytometry was performed to detect NMDA-R in CD45-positive cells from DSS-treated colons positive for CD3, CD103, or Ly6G. CD3-specific antibody detects T cells[34] and, CD3-positive cells demonstrated a bimodal distribution with regard to NMDA-R expression (Figure 4E). Many CD3-positive cells were NMDA-R positive; however, other CD3-positive cells were either NMDA-R negative or expressed low levels of NMDA-R. Bimodal distributions were also observed in

Figure 1 Enzymatically inactive tissue-type plasminogen activator (EI-tPA) reverses colitis in mice treated with 4% dextran sulfate sodium (DSS) for 5 days. **A:** Mice were exposed to 4% DSS in the drinking water for 5 days and then injected with EI-tPA (blue curve) or vehicle (orange curve) intravenously. Control (Con) mice were not exposed to DSS (black curve). Mice that were not exposed to DSS but injected intravenously with EI-tPA are shown with a **dashed black line**. Weight is expressed relative to that recorded on day 0. **B:** Mice were exposed to 4% DSS for 5 days and then treated with EI-tPA or vehicle. Stool scores were determined on the indicated days. **C:** Mice were probed in the lower left quadrant of the abdomen with von Frey filaments to detect sensitivity. Increased response rate to specific filaments reflects increased sensitivity. Cohorts of nine mice were studied, including control mice not exposed to DSS (black circles), mice exposed to 4% DSS for 5 days and tested on day 5 (pink open squares), mice exposed to DSS and tested on day 11 (orange closed squares), and mice exposed to DSS, treated with EI-tPA on day 5, and tested on day 11 (blue triangles). **D:** Representative images of colons harvested from mice that were not DSS exposed (Control), mice exposed to DSS for 5 days and then allowed to recover for 7 days (DSS), and mice exposed to DSS for 5 days, treated with EI-tPA on day 5, and then allowed to recover for 7 days (DSS + EI-tPA). **E:** Colon length results are summarized. **F–H:** Representative hematoxylin and eosin (H&E)–stained sections of colons harvested from mice not exposed to DSS (Control; **F**), mice exposed to 4% DSS for 5 days and then allowed to recover for 7 days (DSS; **G**), and DSS-exposed mice treated once with EI-tPA on day 5 and then allowed to recover for 7 days (DSS + EI-tPA; **H**). **F:** The control colon is marked to show the mucosa (M), which includes epithelium-lined crypts adjacent to the colon lumen, the submucosa (SM), and the muscularis externa (ME). The **arrowheads** indicate the distal ends of the colon sections. **Boxed areas** are shown at higher magnification in the **insets**. **I** and **J:** H&E sections of colons recovered from mice that were not DSS-exposed (Con), exposed to DSS (DSS), and exposed to DSS with subsequent EI-tPA treatment (DSS + EI-tPA) were scored for infiltration of inflammatory cells and epithelial changes in the distal 25% segment. **K:** Sections of colons from mice that were not DSS-exposed (Control) and exposed for 5 days to 4% DSS were immunostained to detect CD11b. High magnification areas are shown in the **insets**. Data are presented as as means ± SEM (**E**, **I**, and **J**). $n = 9$ mice exposed to 4% DSS in the drinking water for 5 days and then injected with EI-tPA or vehicle (**A**); $n = 7$ control mice not exposed to DSS (**A**); $n = 4$ mice not exposed to DSS but injected intravenously with EI-tPA (**A**); $n = 7$ (**E**); $n = 11$ to 14 (**I** and **J**). $^{*}P < 0.05$, $^{**}P < 0.01$, and $^{****}P < 0.0001$ DSS versus DSS + EI-tPA; $^{\dagger\dagger}P < 0.01$, $^{\dagger\dagger\dagger}P < 0.001$ DSS (day 11) versus DSS + EI-tPA; $^{\ddagger}P < 0.05$, $^{\ddagger\ddagger}P < 0.01$, $^{\ddagger\ddagger\ddagger}P < 0.001$, and $^{\ddagger\ddagger\ddagger\ddagger}P < 0.0001$. Scale bars: 1 cm (**D**); 10 μm (**F–H** and **K**, **main images**); 2 μm (**F–H** and **K**, **insets**).

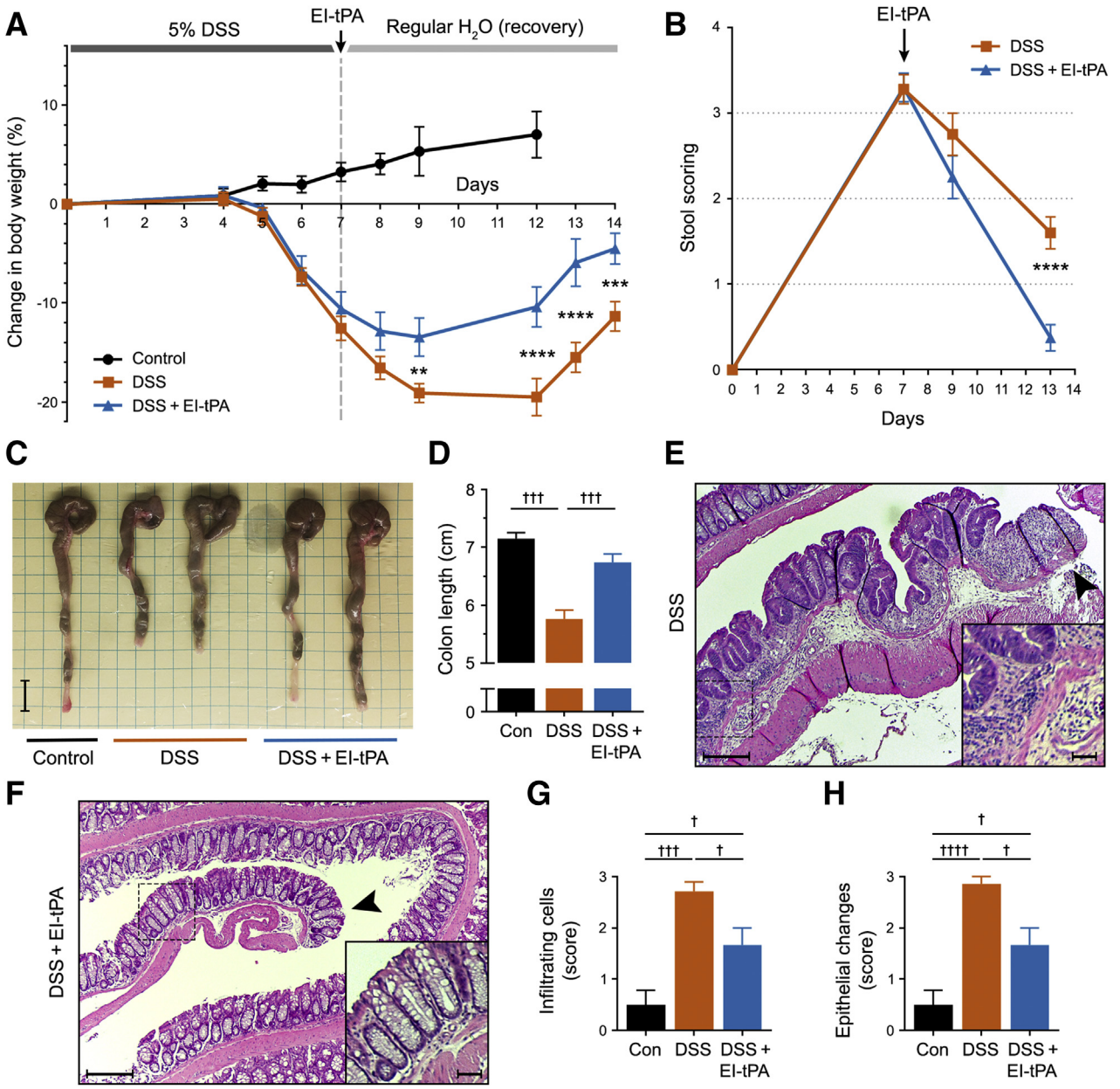

Figure 2 Enzymatically inactive tissue-type plasminogen activator (EI-tPA) reverses colitis in mice exposed to 5% dextran sulfate sodium (DSS) for 7 days. **A:** Mice were exposed to 5% DSS in the drinking water for 7 days and then injected intravenously once with EI-tPA (blue curve) or with vehicle (phosphate-buffered saline; orange curve). Control (Con) mice were not exposed to DSS (black curve). Weight was recorded and expressed as the percentage change compared with that recorded on day 0. **B:** Mice were exposed to 5% DSS for 7 days and then treated with EI-tPA or vehicle. Stool scores were determined on days 7, 9, and 13. **C:** Representative images of colons harvested from mice that were not DSS-exposed (Control), mice exposed to DSS for 7 days and then allowed to recover for 7 days (DSS), and mice exposed to DSS for 7 days, treated with EI-tPA on day 7, and then allowed to recover for 7 days (DSS + EI-tPA). **D:** Colon length results are summarized. **E** and **F:** Representative hematoxylin and eosin (H&E)—stained sections of colons from mice exposed to 5% DSS for 7 days, injected with vehicle on day 7, and allowed to recover for 7 days (**E**) and from mice exposed to DSS, treated with EI-tPA, and then allowed to recover for 7 days (**F**). The **arrowheads** indicate distal ends of the colon sections. **Boxed areas** are shown at higher magnification in the **insets**. **G** and **H:** H&E sections of colons recovered from mice that were not DSS-exposed (Con), exposed to DSS, and exposed to DSS with subsequent EI-tPA treatment were scored for cellular infiltration and for epithelial changes in the distal 25% of the colon. Data are presented as means ± SEM (**D**, **G**, and **H**). $n = 9$ mice exposed to 5% DSS in the drinking water for 7 days and then injected intravenously once with EI-tPA or with vehicle (**A**); $n = 7$ control mice not exposed to DSS (**A**); $n = 7$ (**D**). $^{*}P < 0.05$, $^{**}P < 0.01$, $^{***}P < 0.001$, and $^{****}P < 0.0001$ DSS versus DSS + EI-tPA; $^{\dagger}P < 0.05$, $^{\dagger\dagger\dagger}P < 0.001$, and $^{\dagger\dagger\dagger\dagger}P < 0.0001$. Scale bars: 1 cm (**C**); 10 μm (**E** and **F**, **main images**); 2 μm (**E** and **F**, **insets**).

CD103-positive cells, which include T lymphocytes and dendritic cells,[35] and Ly6G-positive cells, which include mainly neutrophils.[36] Most of the Ly6G-positive cells were NMDA-R-positive. These results suggest that multiple cell types in addition to macrophages may be targets for EI-tPA in colitis.

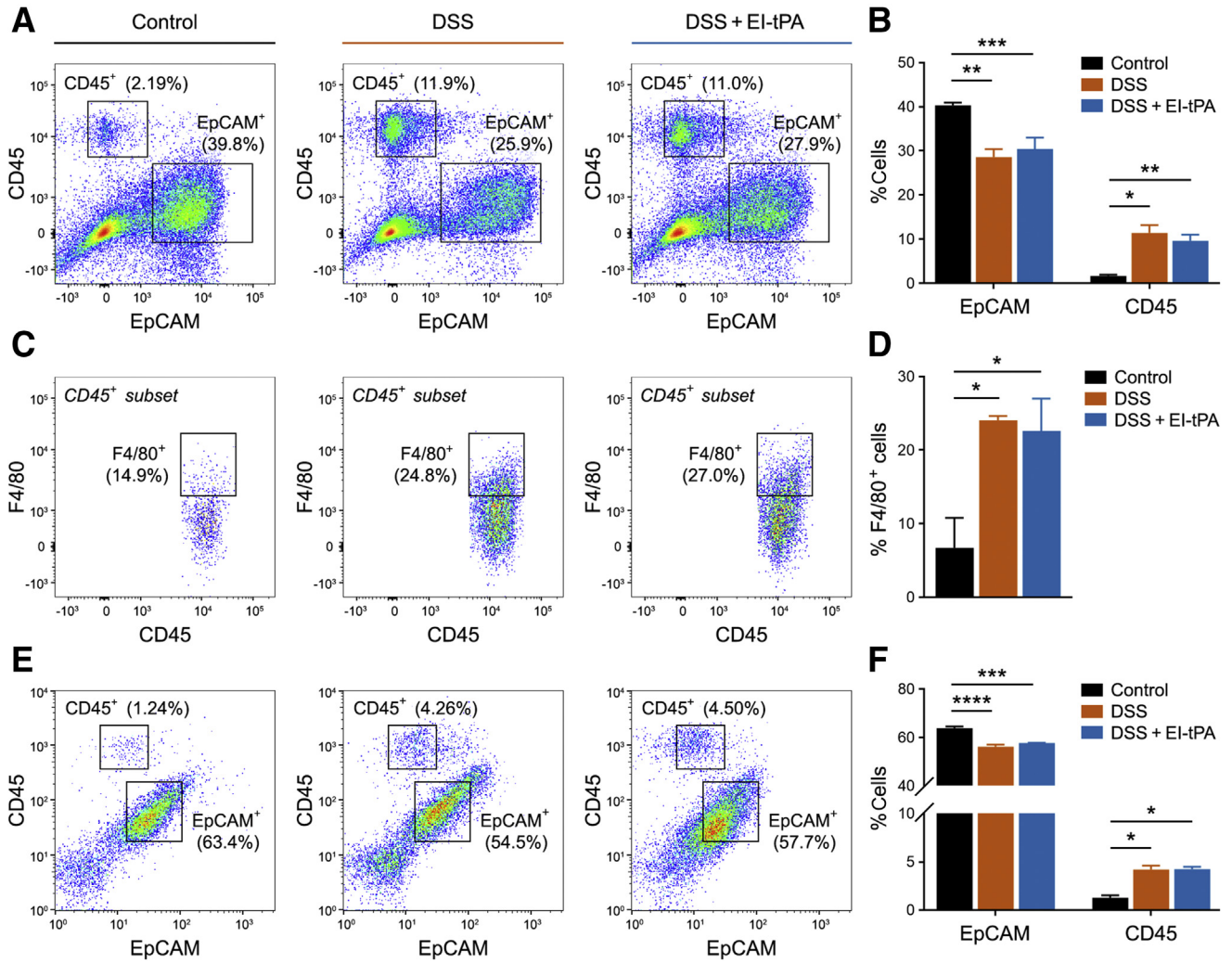

Figure 3 Inflammatory cells in the colon are increased in abundance by dextran sulfate sodium (DSS) but unchanged by enzymatically inactive tissue-type plasminogen activator (EI-tPA). **A:** Representative two-dimensional flow cytometry analyses of epithelial cell adhesion molecule (EpCAM)— and CD45-positive cells harvested by EDTA dissociation from mice not exposed to DSS (Control), mice exposed to 4% DSS for 5 days and then injected with vehicle (DSS), and mice exposed to DSS and then treated with EI-tPA (DSS + EI-tPA). Cells were harvested on day 12, 7 days after terminating DSS treatment. The percentages of cells identified as EpCAM- or CD45-positive, shown in the figure, are for that specific replicate. **B:** Percentages of isolated cells that were EpCAM- and CD45-positive are summarized. **C:** CD45-positive cells were further sorted to determine F4/80-positive cells. A representative study is shown. **D:** F4/80-positive cells are shown as percentages of the CD45-positive cell population. **E:** Representative two-dimensional flow cytometry analyses of EpCAM- and CD45-positive cells in colons that were re-extracted with collagenase. **F:** The percentages of collagenase-dissociated cells that were determined to be EpCAM- and CD45-positive are shown. Data are presented as means ± SEM (**B**, **D**, and **F**); $n = 3$ (**B** and **F**). $^{*}P < 0.05$, $^{**}P < 0.01$, $^{***}P < 0.001$, and $^{****}P < 0.0001$.

Immunohistochemistry was performed to detect LRP1. Clusters of LRP1-immunopositive inflammatory cells were present in the mucosa and submucosa after DSS exposure (Figure 4F). Occasional macrophage-like LRP1-positive cells also were observed in colons from mice not exposed to DSS; however, remarkably, mesenchymal cells that line normal epithelial crypts also appeared to immunostain for LRP1 in control colons. These mesenchymal cells have been implicated in regulating intestinal barrier function and the immune response.[37] EI-tPA treatment restored the pattern of LRP1-expressing cells observed in normal colon to many areas of DSS-exposed colons, especially near the distal end.

Discussion

EI-tPA inhibits and/or reverses proinflammatory responses initiated by TLRs in cultured macrophages.[18,19,22] TLR4 activity is also blocked by EI-tPA *in vivo* in mice,[18] and TLR4 has been implicated in DSS colitis.[38] Thus, we tested the activity of EI-tPA in the DSS model system. DSS colitis is widely accepted as a model system in which innate immunity is a major driver of inflammation.[39] The potential of EI-tPA to counteract inflammation *in vivo* is largely unstudied; however, tPA and EI-tPA express receptor-mediated activities, in addition to effects on TLRs, that may contribute to overall activity in pathologic states, such as DSS colitis. For example,

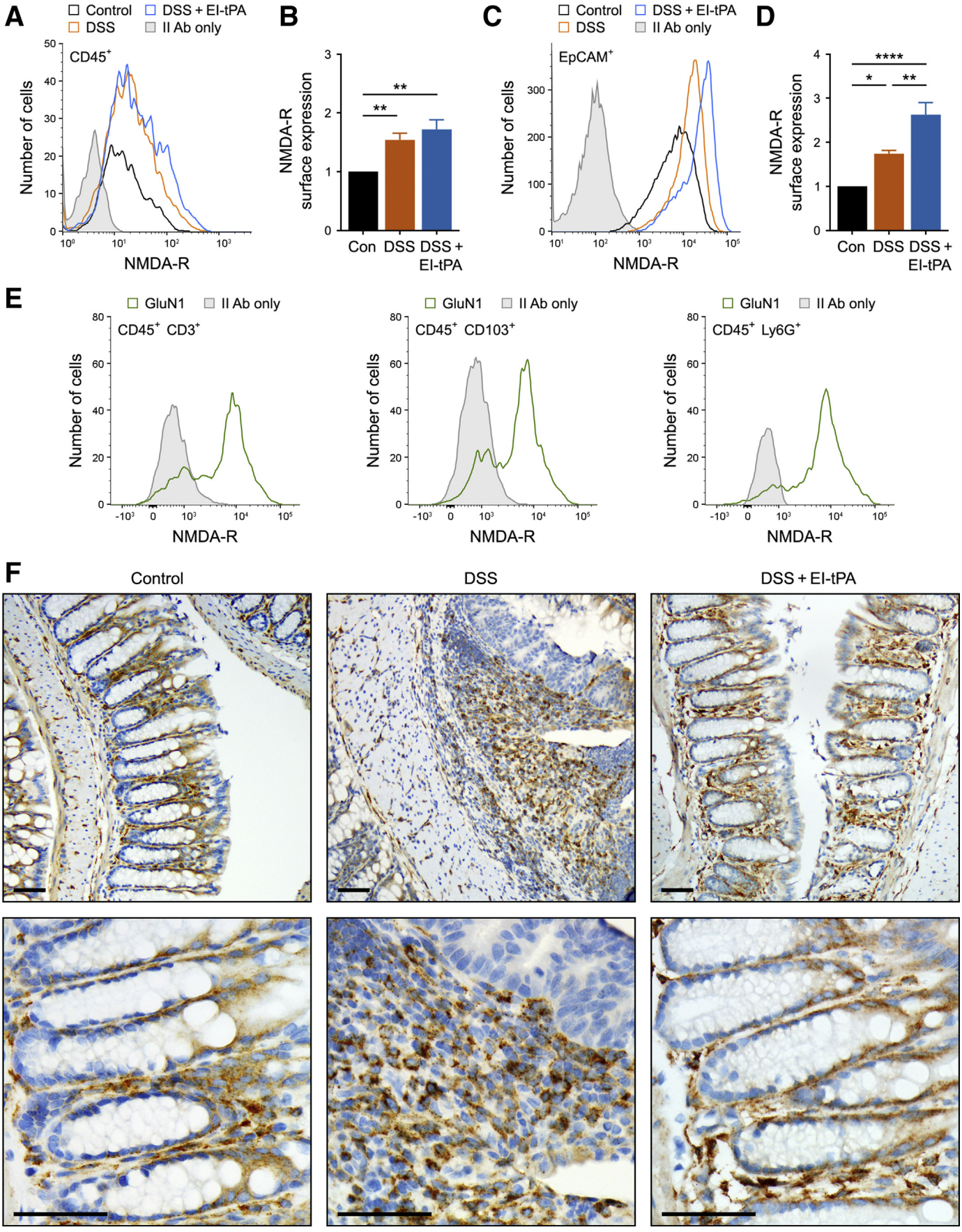
A
Control
DSS
DSS + EI-tPA
II Ab only
CD45+
Number of cells
NMDA-R
B
NMDA-R surface expression
Con
DSS
DSS + EI-tPA
C
EpCAM+
D
E
GluN1
CD45+ CD3+
CD45+ CD103+
CD45+ Ly6G+
F
Control
DSS
DSS + EI-tPA

tPA/EI-tPA and the NMDA-R/LRP1 receptor system promote cell survival[17,40,41] and cell migration.[17,42,43]

To avoid differences in the pathways by which inflammation is established in DSS colitis versus patients with IBD,[23,30] EI-tPA was administered after inflammation was established. An aggressive treatment protocol (5% DSS for 7 days) and a less aggressive protocol (4% DSS for 5 days) was applied. In both cases, a single dose of EI-tPA was administered, and robust evidence of EI-tPA response was observed. EI-tPA significantly accelerated weight recovery and improved stool quality. In the 4% DSS/5 days model system, abdominal tenderness was attenuated in EI-tPA–treated mice. EI-tPA decreased the extent of colon shortening caused by DSS, and histopathologic changes in the distal 25% of the colon improved.

The dose of EI-tPA administered to DSS-treated mice was equivalent to that used previously to reverse the toxicity of lipopolysaccharide in mice,[18] and about 2.5 times the concentration of active tPA administered to patients with stroke.[9] Because EI-tPA is inert in hemostasis, higher doses may be feasible. Interestingly, the circulating half-life of EI-tPA in mice is <5 minutes.[44] This result suggests that EI-tPA rapidly modifies target cells, evoking a sustainable change in their physiology.

Our previous work[18–20,22] suggested that intestinal macrophages may be the target for EI-tPA in DSS-treated mice. However, 7 days after terminating DSS treatment, there was no significant change in the abundance of F4/80-positive macrophage-like cells detected by flow cytometry in EI-tPA–treated mice. Multiple cell types, including intestinal epithelial cells and inflammatory cells, in addition to macrophages, express the NMDA-R, and thus, may have been targets for EI-tPA following induction of DSS colitis. In normal colon, mesenchymal cells surrounding epithelial crypts expressed LRP1. This is important given the emerging role of mesenchymal cells in epithelial barrier function and immune responses.[37] Single-cell transcriptome profiling will be necessary to elucidate target cells for EI-tPA in the DSS model system.

The activity of EI-tPA in rodent models of diseases that involve chronic inflammation has not been well studied. EI-tPA improves the efficacy of induced pluripotent stem cell–derived neural progenitor cells at reversing motor loss following spinal cord injury in rodents.[45] Although inflammation is a factor that influences recovery from spinal cord injury,[46] EI-tPA directly regulated gene expression in the neural progenitor cells via the NMDA-R.[45] Thus, it is not clear whether the positive effects of EI-tPA in this model system resulted in part from anti-inflammatory activity.

This study may be relevant to studies of human IBD patients in which high levels of plasminogen activator inhibitor-1 have been shown to augment tissue damage.[47] Plasminogen activator inhibitor-1 is a rapid inhibitor of the protease activity of tPA.[8] In addition, plasminogen activator inhibitor-1 binding to active tPA blocks the receptor-mediated anti-inflammatory activity of tPA.[48] Mice deficient in the gene that encodes tPA (*PLAT*) demonstrate exacerbated responses to DSS.[47] These results raise the possibility that endogenously produced tPA may regulate IBD progression in patients.

Plasmin also has been shown to exacerbate colitis in the DSS model system, possibly by activating other proteases[49] or by direct proinflammatory cell signaling.[21,22] By studying EI-tPA, the potential confounding effects of plasmin were avoided. Overall, the studies presented herein suggest that the NMDA-R/LRP1 receptor system may be a novel target for drug development in diseases characterized by extensive tissue damage and chronic inflammation.

Acknowledgment

We thank Calvin Lee (University of California San Diego) for advice and technical assistance with flow cytometry studies.

Author Contributions

L.D., M.A.B., and S.L.G. designed the study; L.D., M.A.B., P.A., and D.P. performed the experiments; L.D. and S.L.G. wrote the first draft of the article; all authors interpreted the results and approved the final submission.

Figure 4 Intestinal cells express the tissue-type plasminogen activator (tPA) cell-signaling response system. **A:** Flow cytometry was performed to detect the glutamate ionotropic receptor NMDA type subunit 1 (GluN1) N-methyl-D-aspartate receptor (NMDA-R) subunit in CD45-positive cells isolated from mice exposed to 4% dextran sulfate sodium (DSS) for 5 days and then allowed to recover for 7 days. The mice were treated on day 5 with enzymatically inactive tPA (EI-tPA; DSS + EI-tPA; blue tracing) or with vehicle (DSS; orange tracing). Cells isolated from control (Con) mice that were not DSS-treated are labeled Control (black tracing). GluN1 immunofluorescence is compared with cells stained with secondary antibody only (II Ab only). **B:** The results of six separate flow cytometry studies are summarized. **C:** Flow cytometry was performed to detect the GluN1 NMDA-R subunit in epithelial cell adhesion molecule (EpCAM)–positive cells isolated from mice exposed to 4% DSS for 5 days and then allowed to recover for 7 days. The mice were treated with EI-tPA (DSS + EI-tPA; blue tracing) or with vehicle (DSS; orange tracing). Cells isolated from control mice that were not DSS-treated are labeled Control (black tracing). GluN1 immunofluorescence is compared with cells that were treated with II Ab only. **D:** The results of six separate flow cytometry studies are summarized. **E:** Flow cytometry was performed to detect the GluN1 NMDA-R subunit in CD45-positive cells expressing CD3, CD103, or Ly6G isolated from mice exposed to 4% DSS for 5 days (green tracing; representative of six separate studies). The secondary antibody only control is shown with shaded curves. **F:** Colons were harvested from control mice that were not DSS-exposed and from mice treated with 4% DSS for 5 days, treated with EI-tPA or vehicle, and allowed to recover for 7 days. Immunohistochemistry for low-density lipoprotein receptor–related protein-1 was performed. Data are presented as means ± SEM (**B** and **D**). $^{*}P < 0.05$, $^{**}P < 0.01$, and $^{****}P < 0.0001$. Scale bars = 50 μm (**F**).

References

1. De Souza HSP, Fiocchi C: Immunopathogenesis of IBD: current state of the art. Nat Rev Gastroenterol Hepatol 2016, 13:13−27
2. Hugot JP, Chamaillard M, Zouali H, Lesage S, Cézard JP, Belaiche J, Almer S, Tysk C, O'morain CA, Gassull M, Binder V, Finkel Y, Cortot A, Modigliani R, Laurent-Puig P, Gower-Rousseau C, Macry J, Colombel JF, Sahbatou M, Thomas G: Association of NOD2 leucine-rich repeat variants with susceptibility to Crohn's disease. Nature 2001, 411:599−603
3. Vindigni SM, Zisman TL, Suskind DL, Damman CJ: The intestinal microbiome, barrier function, and immune system in inflammatory bowel disease: a tripartite pathophysiological circuit with implications for new therapeutic directions. Therap Adv Gastroenterol 2016, 9: 606−625
4. Morgan XC, Tickle TL, Sokol H, Gevers D, Devaney KL, Ward DV, Reyes JA, Shah SA, LeLeiko N, Snapper SB, Bousvaros A, Korzenik J, Sands BE, Xavier RJ, Huttenhower C: Dysfunction of the intestinal microbiome in inflammatory bowel disease and treatment. Genome Biol 2012, 13:R79
5. Kostic AD, Xavier RJ, Gevers D: The microbiome in inflammatory bowel disease: current status and the future ahead. Gastroenterology 2014, 146:1489−1499
6. Neurath MF: Current and emerging therapeutic targets for IBD. Nat Rev Gastroenterol Hepatol 2017, 14:269−278
7. Castellino FJ, Ploplis VA: Structure and function of the plasminogen/plasmin system. Thromb Haemost 2005, 93:647−654
8. Cesarman-Maus G, Hajjar KA: Molecular mechanisms of fibrinolysis. Br J Haematol 2005, 129:307−321
9. Albers GW, Bates VE, Clark WM, Bell R, Verro P, Hamilton SA: Intravenous tissue-type plasminogen activator for treatment of acute stroke: the standard treatment with alteplase to reverse stroke (STARS) study. J Am Med Assoc 2000, 283:1145−1150
10. van Zonneveld A-J, Veerman H, MacDonald ME, Pannekoek H, van Mourik JA: Structure and function of human tissue-type plasminogen activator (t-PA). J Cell Biochem 1986, 32:169−178
11. Ny T, Elgh F, Lund B: The structure of the human tissue-type plasminogen activator gene: correlation of intron and exon structures to functional and structural domains. Proc Natl Acad Sci U S A 1984, 81:5355−5359
12. Bennett WF, Paoni NF, Keyt BA, Botstein D, Jones AJS, Presta L, Wurm FM, Zoller MJ: High resolution analysis of functional determinants on human tissue-type plasminogen activator. J Biol Chem 1991, 266:5191−5201
13. Fernández-Monreal M, López-Atalaya JP, Benchenane K, Cacquaevel M, Dulin F, Le Caer JP, Rossier J, Jarrige AC, MacKenzie ET, Colloc'h N, Ali C, Vivien D: Arginine 260 of the amino-terminal domain of NR1 subunit is critical for tissue-type plasminogen activator-mediated enhancement of N-methyl-D-aspartate receptor signaling. J Biol Chem 2004, 279:50850−50856
14. Samson AL, Nevin ST, Croucher D, Niego B, Daniel PB, Weiss TW, Moreno E, Monard D, Lawrence DA, Medcalf RL: Tissue-type plasminogen activator requires a co-receptor to enhance NMDA receptor function. J Neurochem 2008, 107:1091−1101
15. Martin AM, Kuhlmann C, Trossbach S, Jaeger S, Waldron E, Roebroek A, Luhmann HJ, Laatsch A, Weggen S, Lessmann V, Pietrzik CU: The functional role of the second NPXY motif of the LRP1 β-chain in tissue-type plasminogen activator-mediated activation of N-methyl-D-aspartate receptors. J Biol Chem 2008, 283: 12004−12013
16. Mantuano E, Lam MS, Gonias SL: LRP1 assembles unique co-receptor systems to initiate cell signaling in response to tissue-type plasminogen activator and myelin-associated glycoprotein. J Biol Chem 2013, 288:34009−34018
17. Mantuano E, Lam MS, Shibayama M, Marie Campana W, Gonias SL: The NMDA receptor functions independently and as an LRP1 co-receptor to promote Schwann cell survival and migration. J Cell Sci 2015, 128:3478−3488
18. Mantuano E, Azmoon P, Brifault C, Banki MA, Gilder AS, Campana WM, Gonias SL: Tissue-type plasminogen activator regulates macrophage activation and innate immunity. Blood 2017, 130: 1364−1374
19. Das L, Azmoon P, Banki MA, Mantuano E, Gonias SL: Tissue-type plasminogen activator selectively inhibits multiple toll-like receptors in CSF-1 differentiated macrophages. PLoS One 2019, 14:e0224738
20. Mantuano E, Brifault C, Lam MS, Azmoon P, Gilder AS, Gonias SL: LDL receptor-related protein-1 regulates NFκB and microRNA-155 in macrophages to control the inflammatory response. Proc Natl Acad Sci U S A 2016, 113:1369−1374
21. Syrovets T, Jendrach M, Rohwedder A, Schüle A, Simmet T: Plasmin-induced expression of cytokines and tissue factor in human monocytes involves AP-1 and IKKβ-mediated NF-κB activation. Blood 2001, 97:3941−3950
22. Zalfa C, Azmoon P, Mantuano E, Gonias SL: Tissue-type plasminogen activator neutralizes LPS but not protease-activated receptor-mediated inflammatory responses to plasmin. J Leukoc Biol 2019, 105:729−740
23. Hogan-Cann AD, Anderson CM: Physiological roles of non-neuronal NMDA receptors. Trends Pharmacol Sci 2016, 37:750−767
24. Mehra A, Guérit S, Macrez R, Gosselet F, Sevin E, Lebas H, Maubert E, de Vries HE, Bardou I, Vivien D, Docagne F: Non-ionotropic action of endothelial NMDA receptors on blood−brain barrier permeability via Rho/ROCK-mediated phosphorylation of myosin. J Neurosci 2020, 40:1778−1787
25. Perše M, Cerar A: Dextran sodium sulphate colitis mouse model: traps and tricks. J Biomed Biotechnol 2012, 2012:13
26. Laird JMA, Martinez-Caro L, Garcia-Nicas E, Cervero F: A new model of visceral pain and referred hyperalgesia in the mouse. Pain 2001, 92:335−342
27. Erben U, Loddenkemper C, Doerfel K, Spieckermann S, Haller D, Heimesaat MM, Zeitz M, Siegmund B, Kühl AA: A guide to histomorphological evaluation of intestinal inflammation in mouse models. Int J Clin Exp Pathol 2014, 7:4557−4576
28. Lin HH, Faunce DE, Stacey M, Terajewicz A, Nakamura T, Zhang-Hoover J, Kerley M, Mucenski ML, Gordon S, Stein-Streilein J: The macrophage F4/80 receptor is required for the induction of antigen-specific efferent regulatory T cells in peripheral tolerance. J Exp Med 2005, 201:1615−1625
29. Traynelis SF, Wollmuth LP, McBain CJ, Menniti FS, Vance KM, Ogden KK, Hansen KB, Yuan H, Myers SJ, Dingledine R: Glutamate receptor ion channels: structure, regulation, and function. Pharmacol Rev 2010, 62:405−496
30. Cooper HS, Murthy SNS, Shah RS, Sedergran DJ: Clinicopathologic study of dextran sulfate sodium experimental murine colitis. Lab Investig 1993, 69:238−250
31. Mazzone A, Ricevuti G: Leukocyte CD11/CD18 integrins: biological and clinical relevance. Haematologica 1995, 80:161−175
32. Kinchen J, Chen HH, Parikh K, Antanaviciute A, Jagielowicz M, Fawkner-Corbett D, Ashley N, Cubitt L, Mellado-Gomez E, Attar M, Sharma E, Wills Q, Bowden R, Richter FC, Ahern D, Puri KD, Henault J, Gervais F, Koohy H, Simmons A: Structural remodeling of the human colonic mesenchyme in inflammatory bowel disease. Cell 2018, 175:372−386
33. Hu K, Yang J, Tanaka S, Gonias SL, Mars WM, Liu Y: Tissue-type plasminogen activator acts as a cytokine that triggers intracellular signal transduction and induces matrix metalloproteinase-9 gene expression. J Biol Chem 2006, 281:2120−2127
34. Janeway CA: The T cell receptor as a multicomponent signalling machine: CD4/CD8 coreceptors and CD45 in T cell activation. Annu Rev Immunol 1992, 10:645−674
35. Johansson-Lindbom B, Svensson M, Pabst O, Palmqvist C, Marquez G, Förster R, Agace WW: Functional specialization of gut

CD103+ dendritic cells in the regulation of tissue-selective T cell homing. J Exp Med 2005, 202:1063–1073
36. Lee PY, Wang J-X, Parisini E, Dascher CC, Nigrovic PA: Ly6 family proteins in neutrophil biology. J Leukoc Biol 2013, 94:585–594
37. Nowarski R, Jackson R, Flavell RA: The stromal intervention: regulation of immunity and inflammation at the epithelial-mesenchymal barrier. Cell 2017, 168:362–375
38. Fukata M, Michelsen KS, Eri R, Thomas LS, Hu B, Lukasek K, Nast CC, Lechago J, Xu R, Naiki Y, Soliman A, Arditi M, Abreu MT: Toll-like receptor-4 is required for intestinal response to epithelial injury and limiting bacterial translocation in a murine model of acute colitis. Am J Physiol Gastrointest Liver Physiol 2005, 288:51–55
39. Kiesler P, Fuss IJ, Strober W: Experimental models of inflammatory bowel diseases. Cell Mol Gastroenterol Hepatol 2015, 1:154–170
40. Echeverry R, Wu J, Haile WB, Guzman J, Yepes M: Tissue-type plasminogen activator is a neuroprotectant in the mouse hippocampus. J Clin Invest 2010, 120:2194–2205
41. Campana WM, Li X, Dragojlovic N, Janes J, Gaultier A, Gonias SL: The low-density lipoprotein receptor-related protein is a pro-survival receptor in Schwann cells: possible implications in peripheral nerve injury. J Neurosci 2006, 26:11197–11207
42. Cao C, Lawrence DA, Li Y, Von Arnim CAF, Herz J, Su EJ, Makarova A, Hyman BT, Strickland DK, Zhang L: Endocytic receptor LRP together with tPA and PAI-1 coordinates Mac-1-dependent macrophage migration. EMBO J 2006, 25:1860–1870
43. Achuta VS, Rezov V, Uutela M, Louhivuori V, Louhivuori L, Castrén ML: Tissue plasminogen activator contributes to alterations of neuronal migration and activity-dependent responses in fragile X mice. J Neurosci 2014, 34:1916–1923
44. Fuchs HE, Berger H, Pizzo SV: Catabolism of human tissue plasminogen activator in mice. Blood 1985, 65:539–544
45. Shiga Y, Shiga A, Mesci P, Kwon HJ, Brifault C, Kim JH, Jeziorski JJ, Nasamran C, Ohtori S, Muotri AR, Gonias SL, Campana WM: Tissue-type plasminogen activator-primed human iPSC-derived neural progenitor cells promote motor recovery after severe spinal cord injury. Sci Rep 2019, 9:19291
46. Fitch MT, Silver J: CNS injury, glial scars, and inflammation: inhibitory extracellular matrices and regeneration failure. Exp Neurol 2008, 209:294–301
47. Kaiko GE, Chen F, Lai CW, Chiang IL, Perrigoue J, Stojmirović A, Li K, Muegge BD, Jain U, VanDussen KL, Goggins BJ, Keely S, Weaver J, Foster PS, Lawrence DA, Liu TC, Stappenbeck TS: PAI-1 augments mucosal damage in colitis. Sci Transl Med 2019, 11: eaat0852
48. Gonias SL, Banki MA, Gilder AS, Azmoon P, Campana WM, Mantuano E: PAI1 blocks NMDA receptor-mediated effects of tissue-type plasminogen activator on cell signaling and physiology. J Cell Sci 2018, 131:jcs217083
49. Munakata S, Tashiro Y, Nishida C, Sato A, Komiyama H, Shimazu H, Dhahri D, Salama Y, Eiamboonsert S, Takeda K, Yagita H, Tsuda Y, Okada Y, Nakauchi H, Sakamoto K, Heissig B, Hattori K: Inhibition of plasmin protects against colitis in mice by suppressing matrix metalloproteinase 9-mediated cytokine release from myeloid cells. Gastroenterology 2015, 148:565–578.e4